Superconducting critical temperature T_c and electronic structure of pseudoternary $Y(Rh_{1-x}Ru_x)_4B_4$ studied by high-resolution photoelectron spectroscopy

R. Knauf, H. Adrian, and A. Meinelt
Physikalisches Institut der Universität Erlangen—Nürnberg, Erwin-Rommel-Strasse 1, D-8520 Erlangen, Federal Republic of Germany

R. L. Johnson
Max-Planck Institut für Festkörperforschung, Heisenbergstrasse 1, D-7000 Stuttgart 80, Federal Republic of Germany
(Received 18 March 1985)

High-resolution photoemission measurements using synchrotron radiation are presented for the body-centered-tetragonal superconducting pseudoternary system $Y(Rh_{1-x}Ru_x)_4B_4$ covering the range of composition $0.10 \leq x \leq 0.90$. The superconducting phase diagram determined down to 4 mK reproduces the sharp drop in the superconducting critical temperature T_c for $x > x_{cr} = 0.35$, which is characteristic for this class of compound. No superconductivity was observed for the sample with $x = 0.70$, whereas the sample with $x = 0.90$ became superconducting again at $T_c = 140$ mK. From a comparison between the valence-band spectra near the Fermi level E_F and band-structure calculations by Jarlborg *et al.* for the related compounds MRh_4B_4 with M = Y, Gd, Ho, Er, and Lu, we conclude that a shift of E_F to lower energies with increasing x is the underlying mechanism for the $T_c(x)$ behavior. In our previous study on $Ho(Rh_{1-x}Ru_x)_4B_4$, for which supplementary data are also presented, the same features were observed. Our measurements indicate that hybridization effects upon alloying Ru for Rh cannot explain the observed behavior of T_c.

I. INTRODUCTION

The occurrence of superconductivity and magnetic ordering phenomena in ternary transition-metal borides has recently attracted the interest of many experimentalists and theorists.[1,2] The study of pseudoternary systems $R(Rh_{1-x}T_x)_4B_4$ (R = Gd, Tb, Dy, Ho, Er, Tm, Lu, and Y; T = Ru and Ir)[3–9] revealed an unexpected drastic decrease of T_c in a close interval Δx of the composition parameter x (typically $\Delta x = 0.10$) near a critical concentration x_{cr} (typically $x_{cr} = 0.35$—0.50). This general feature was found for quite different systems. It is observed for two different modifications of the crystal structure [body centered tetragonal (bct) and primitive tetragonal (pt)], with magnetic and nonmagnetic R atoms, and with transition metals T which either reduce the number of valence electrons or leave it constant. The qualitatively universal occurrence of the drastic T_c decrease in all these different cases has led to speculations that a universally applicable mechanism should be responsible.

In recent papers[4,9] we presented high-resolution photoemission measurements which conclusively show that in the two systems $Ho(Rh_{1-x}Ru_x)_4B_4$ and $Ho(Rh_{1-x}Ir_x)_4B_4$ the substitution of Rh by the transition metals Ru and Ir has completely different effects on the electronic valence-band structure. Nevertheless, in the framework of existing band-structure calculations both should cause a T_c depression which is qualitatively consistent with the experimental T_c data. In the case of $Ho(Rh_{1-x}Ru_x)_4B_4$ the width of the d-band structure close to E_F remains nearly constant and the measured spectra show that the effect of substitution can be described in a rigid-band model by a shift of the Fermi level E_F to lower energies with increasing x due to a reduction of the d-valence electron concentration.

The details of valence-band spectra near E_F indicate in agreement with band-structure calculations that for higher values of x the shift of E_F causes a significant reduction of the electronic density of states $N(E_F)$ resulting in a strong decrease of T_c. Contrary to this for $Ho(Rh_{1-x}Ir_x)_4B_4$ a broadening of the d-band structure is observed, originating from an increasing overlap of the more extended $5d$ wave function of Ir. A numerical simulation of this broadening according to the experimental data implies that the restriction to a constant number of occupied states leads to a shift of E_F to higher energies if the broadening exceeds a certain level. The consequence is again a decrease of $N(E_F)$ and hence T_C.

In order to investigate whether the outlined mechanisms are also valid for other pseudoternary systems a detailed study of bct $Y(Rh_{1-x}Ru_x)_4B_4$ was performed. Additional data for $Ho(Rh_{1-x}Ru_x)_4B_4$ are also presented. Furthermore, a comparison of these two systems provides information about the influence of the R-atom sublattice.

II. EXPERIMENTAL

The samples covering the range of composition from $x = 0.10$ to $x = 0.90$ were prepared by arc-melting in a zirconium-gettered argon atmosphere. First the Rh/Ru ratio was fixed by melting stoichiometric amounts of rhodium and ruthenium ingots together. Then appropriate pieces of boron were successively melted in. In a final step the correct mass of yttrium was added. To improve homogeneity the ingots were remelted several times. After this procedure the typical total mass losses during

arc-melting were about 0.5 wt. %. For all samples the powder x-ray diffraction patterns obtained with monochromatized Cu $K\alpha$ radiation can be indexed with the body-centered-tetragonal structure reported by Johnston.[7] Only in two cases ($x=0.50$ and 0.70) were small amounts of RhB as an impurity phase detected. The superconducting phase diagram was determined by measuring the ac-susceptibility using a mutual-inductance bridge operating at 27 Hz in a ^{4}He-bath cryostat and a ^{3}He-^{4}He dilution refrigerator down to 4 mK. Temperatures down to 1.3 K were measured by a calibrated carbon-glass resistor, down to about 50 mK by a calibrated germanium resistor, and below 50 mK a ^{60}Co nuclear orientation thermometer was used as a temperature standard.

For the photoemission measurements the nearly spherical samples of about 0.7 g were cut into four pieces resulting in a surface of semicircular shape of about 5 mm in diameter. The spectra were recorded in an ultrahigh-vacuum system with a total base pressure of 4×10^{11} mbar. Electron energy analysis utilized a double-pass cylindrical mirror analyzer (PHI) at a fixed pass energy. Synchrotron radiation from the DORIS storage ring in Hamburg was employed, monochromatized by a high-resolution grating monochromator. Details of the apparatus are reported elsewhere.[10] The total experimental resolution determined by measuring the molybdenum Fermi edge was found to be 0.25 and 0.33 eV at $h\nu=21.6$ and 60 eV, respectively. For $h\nu\geq100$ eV the analyzer pass energy was increased so that the total resolution was 0.8 eV.

The samples were cleaned by repeated scraping *in situ* with a diamond file. After cleaning no traces of carbon or oxygen could be detected. Cleaning of the samples by scraping was preferred to ion bombardment in order to avoid changes in surface composition.

III. RESULTS AND DISCUSSION

A. Phase diagram

Figure 1 shows the superconducting critical temperatures T_c for $Y(Rh_{1-x}Ru_x)_4B_4$ including the data reported by Shelton *et al.*[8] In their measurements they found $x_{cr}=0.32$ for annealed samples and $x_{cr}=0.50$ for arc-melted samples. The superconducting critical temperatures for arc-melted samples presented in this work ($x_{cr}=0.35$) are between those of the two sets of samples mentioned above. We therefore conclude that the microscopic state of our samples with regard to the annealing treatment is intermediate, which might be due to a smaller cooling rate of the copper hearth of our arc-furnace. However, the general behavior is quite similar. T_c remains nearly constant for $x\leq x_{cr}$. For higher values of x a sharp decrease of T_c is observed. For the sample with $x=0.70$ no superconducting transition could be detected down to 4 mK, while the sample with $x=0.90$ becomes superconducting again at $T_c=140$ mK. The superconducting transition widths are in the range 110–220 mK for $x\leq x_{cr}$ and increase up to 1100 mK for $x=0.50$, whereas the sample with $x=0.90$ again reveals a rather sharp transition with a transition width of 150 mK. With the exception of the reoccurrence of superconductivity for $x\geq0.90$, the superconducting phase diagrams of $Y(Rh_{1-x}Ru_x)_4B_4$ and $Ho(Rh_{1-x}Ru_x)_4B_4$ are qualitatively extremely similar. The presence of magnetic ions occupying a regular sublattice in the case of $Ho(Rh_{1-x}Ru_x)_4B_4$ has two main effects. These are magnetic ordering phenomena at very low temperatures[11] and an overall reduction of T_c presumably due to exchange interaction between the $4d$ conduction electrons and the localized $4f$ electrons. However, the abrupt decrease of T_c close to a critical concentration of Ru, about which we are mainly concerned in this study, appears not to be influenced at all by magnetic ions.

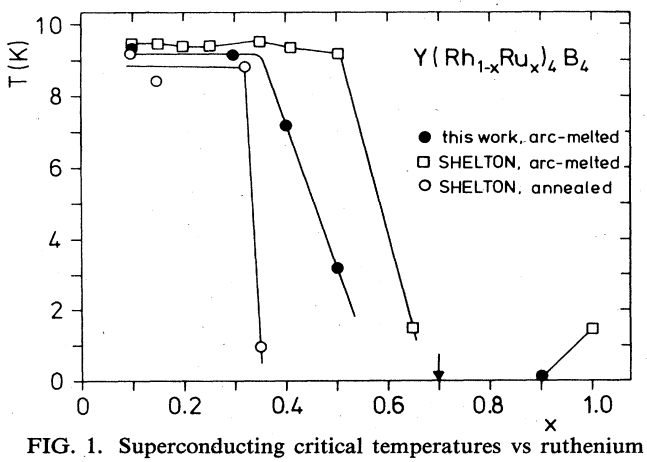

FIG. 1. Superconducting critical temperatures vs ruthenium concentration x for $Y(Rh_{1-x}Ru_x)_4B_4$. The open circles are taken from Ref. 8. The arrow for the sample with $x=0.70$ indicates that no superconducting transition was observed down to 4 mK. The lines are drawn as a guide to the eye.

B. Photoemission spectra

The upper curve of Fig. 2(a) shows the valence-band spectrum of $Y(Rh_{0.90}Ru_{0.10})_4B_4$ recorded at $h\nu=60$ eV. Significant features of this spectrum are a strong peak at 1.8 eV and two smaller ones at 8.4 eV and 10.6 eV binding energies E_B, respectively. All energies are referred to the Fermi level E_F. Furthermore a shoulder near $E_B=4.2$ eV is detectable.

To correct the spectrum for the contribution of inelastically scattered electrons a background subtraction procedure was applied which is described in detail in Ref. 12. The underlying idea is that the background BG at an energy E is proportional to the number of electrons with energies larger than E. This is a reasonable assumption because only those electrons with an energy higher than E are able to contribute via inelastic scattering to the background at the energy E. The result of this background calculation is also shown in Fig. 2(a), where the dashed line represents the contribution of inelastically scattered electrons and the lower curve the spectrum after background subtraction. After magnification by a factor of 10 the two peaks at $E_B=8.4$ eV and 10.6 eV are clearly visible.

Valuable insight in the origin of these peaks can be obtained by comparing the spectra with band-structure calculations by Jarlborg *et al.*[13–15] for the related compounds RRh_4B_4, where $R=$Y, Gd, Ho, Er, and Lu. The

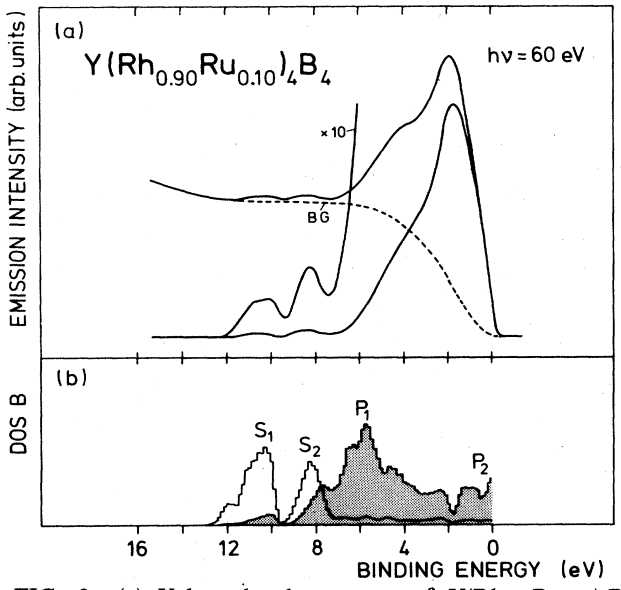

FIG. 2. (a) Valence-band spectrum of $Y(Rh_{0.90}Ru_{0.10})_4B_4$ (upper curve). The lower curve is obtained after subtracting the background BG of inelastically scattered electrons (dashed line). (b) Calculated l-decomposed DOS for B in $HoRh_4B_4$ (from Ref. 15).

published data for the energy dependence of the density of states (DOS) for pt $HoRh_4B_4$ and pt $ErRh_4B_4$ should also be a good representation of the electronic structure of $Y(Rh_{1-x}Ru_x)_4B_4$ for several reasons. First, the calculations show that the s, p, and d contributions from the rare-earth site are small while the contributions from localized $4f$ states are not taken into account for the calculation of the total DOS.[15] In the case of trivalent yttrium (which has a noble-gas-like electronic configuration) in $Y(Rh_{1-x}Ru_x)_4B_4$ no significant emission in the valence-band region is expected either. A possible objection could be that these calculations are performed for the $CeCo_4B_4$-type structure rather than the body-centered tetragonal (bct) lattice of $Y(Rh_{1-x}Ru_x)_4B_4$. However, the only distinction between these two structure types consists of a different orientation of half of the transition metal and boron tetrahedra which should have only an insignificant effect on the energy of the strongly localized d bands, and therefore on the electronic density of states. This we have demonstrated in photoemission measurements on bct $Ho(Rh_{1-x}Ru_x)_4B_4$.[9]

The calculated boron partial DOS is shown in Fig. 2(b). The peak s_1 originates from atomic boron s states while s_2 is supposed to correspond to transition-metal p states that spill over with $l=0$ character into the boron muffin tins. p_1 and p_2 have been attributed to pd hybrid components.[16] For the comparison with the experimental data E_F is shifted upward 1 eV. This shift is exactly the same as the value of the empirical shift given by Hamaker *et al.*[8,16,17] to fit their Auger data on $Y(Rh_{1-x}Ru_x)_4B_4$, and is possibly caused by slightly different charge transfer effects which have been shown to be important in the self-consistent calculations.[15] The agreement between Fig.

TABLE I. Binding energies E_B in eV of the valence-band features s_1 and s_2 in RhB, RuB, IrB, and $Y(Rh_{0.90}Ru_{0.10})_4B_4$, relative to the Fermi level E_F.

Peak	s_1	s_2
RhB	8.6±0.1	10.9±0.1
RuB	8.6±0.1	10.8±0.1
IrB	8.8±0.1	10.5±0.1
$Y(Rh_{0.90}Ru_{0.10})_4B_4$	8.4±0.1	10.6±0.1

2(a) and Fig. 2(b) concerning peak s_1 and s_2 is excellent so that these peaks with $E_B=8.4$ and 10.6 eV, respectively, can be attributed to the boron states. This identification is further supported by measurements on RhB, RuB, and IrB. In Table I the binding energies of the peaks labeled s_1 and s_2 are listed. Although the d-band structure of these compounds is quite different, the values for the binding energies of s_1 and s_2 are nearly identical.

In Fig. 3 the calculated l-decomposed partial density of states at the Rh site for $HoRh_4B_4$ is shown (from Ref. 15). There are three strong peaks at $E_B=1.6$, 2.5, and 4.7 eV originating from Rh $4d$ states. These values are close to those calculated by Smith *et al.*[18] (1.3, 2.5, and 5.1 eV) as well as x-ray and ultraviolet photoemission spectroscopy data[18–20] for Rh metal. In conjunction with Fig. 2(b) it can therefore be concluded that the shoulder around 4.2 eV in the $Y(Rh_{1-x}Ru_x)_4B_4$ spectra [see Fig. 2(a)] is an unresolved superposition of mainly Rh d states in the upper part and B p_1 states ($E_B=5.9$ eV) in the lower part

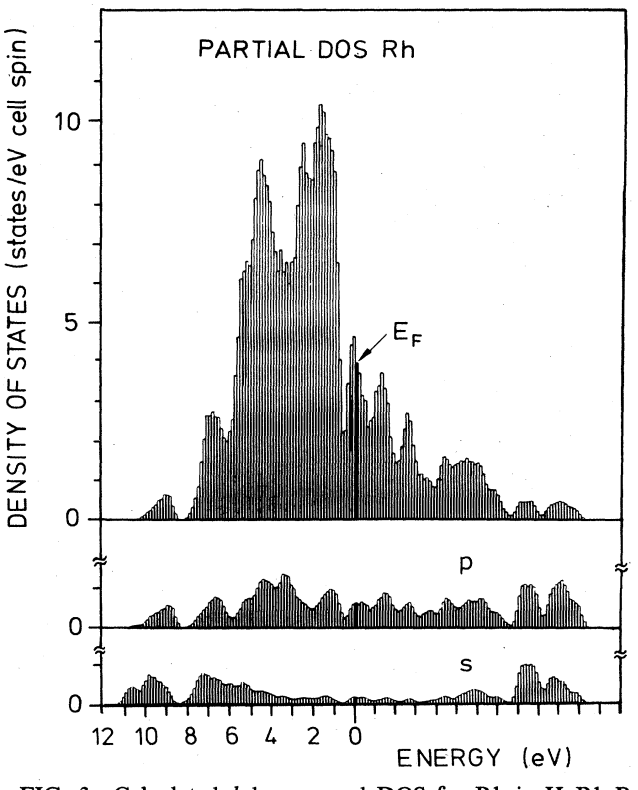

FIG. 3. Calculated l-decomposed DOS for Rh in $HoRh_4B_4$ (from Ref. 15).

of this shoulder. The peak at $E_B=1.8$ eV in Fig. 2(a) appears entirely due to Rh $4d$ electrons.

In Fig. 4 a set of valence-band spectra ($x=0.40$) is shown for different photon energies $h\nu=21-120$ eV, aligned with respect to E_F. Upon increasing the photon energy from $h\nu=21$ eV to $h\nu=40$ eV an increase of the relative emission intensity of the peak at $E_B=1.8$ eV is detectable. After a minimum around $h\nu=50$ eV a distinct maximum of the relative emission intensity occurs at $h\nu=60$ eV. For higher photon energies a strong decrease is observed. The same dependence of the photoemission cross section of the corresponding structure was found for $Ho(Rh_{1-x}Ru_x)_4B_4$.[9] This, in conjunction with optical-absorption measurements[21] on Rh metal, further supports the identification of this peak as transition-metal d band. Upon varying the photon energy from $h\nu=60$ to 120 eV the initial shoulder at $E_B=4.2$ eV develops into a peak at $E_B=5$ eV ($h\nu=90$ eV), which then shifts to $E_B=6$ eV.

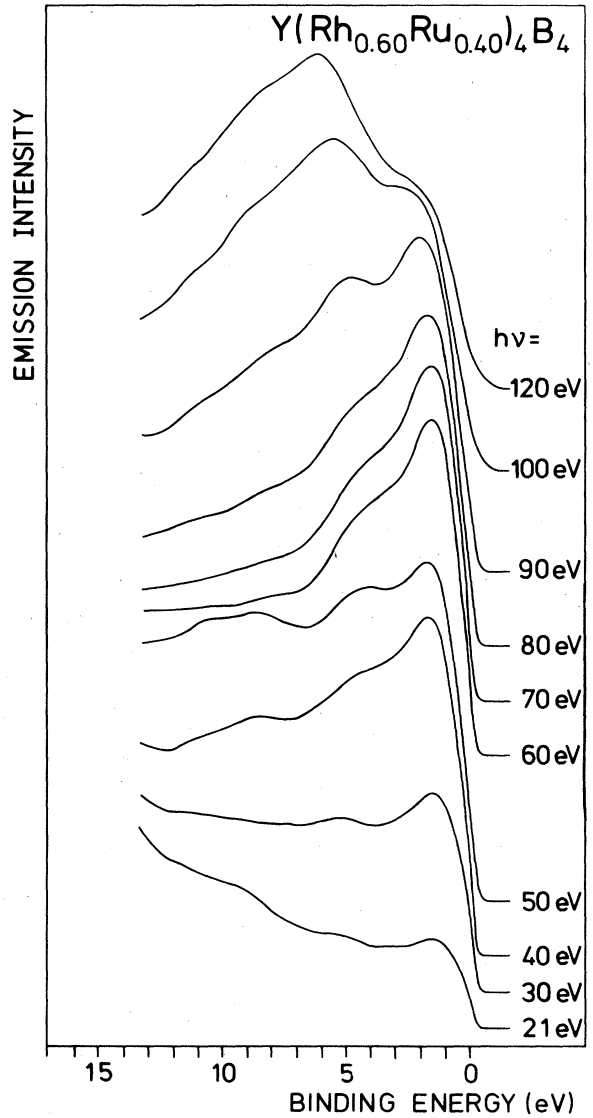

FIG. 4. Valence-band spectra of $Y(Rh_{0.60}Ru_{0.40})_4B_4$ for different photon energies.

The reason for this behavior is the decrease of emission intensity of the transition-metal d-band structure at higher photon energies so that the boron p_1 states ($E_B=5.9$ eV) which cannot be resolved for $h\nu<80$ eV are dominant in this region of binding energy at $h\nu=120$ eV. It should be emphasized that there is an excellent agreement between the measured binding energy of the boron p_1 states and the value given by the shifted density-of-states calculation further justifying the 1-eV correction of the energy scale made in Fig. 2(b).

The spectrum at $h\nu=21$ eV shown in Fig. 4 contrasts with those reported by Hamaker *et al.*[16,17] Their He I photoemission data reveal transition-metal d-band emission around $E_B=1.7$ eV, a strong peak at $E_B=5.8$ eV, and a shoulder at $E_B=8.5$ eV. The latter were interpreted originating from boron p_1 and s_2 states, respectively. No emission from boron s_1 states was found. Unfortunately, no raw data but only spectra after spline-generated background removal were displayed. Nevertheless, in no case could we find such pronounced structures with binding energies of about 5.8 eV and 8.6 eV at $h\nu=21$ eV. If a reasonable background is assumed the dominant feature in our data turns out to be the transition-metal d band at binding energy equal to 1.8 eV. Weak structures at binding energies equal to 3.0 and 5 eV can be attributed to additional d-band emission. Evidence for both boron s_1 and s_2 emission is discernible. However, the binding-energy values seem to be increased due to the steep increase of the background curve. Although we cannot give a conclusive explanation for the discrepancy which mainly consists in the lack of pronounced peaks at $E_B=5.8$ and 8.5 eV in our data, two possibilities are conceivable. One is the presence of residual oxygen impurities which the authors of Ref. 17 detected in their Auger measurements, although one would not expect in this case the observed systematic dependence on stoichiometry. As a second possibility one has to consider the background subtraction procedure in Refs. 16 and 17, where only photoemission spectra after background removal are presented.

In our previous study on bct pseudoternary $Ho(Rh_{1-x}Ru_x)_4B_4$ we gave conclusive evidence that the substitution of Ru for Rh in that system causes a shift of E_F relative to the d-band structure. This shift leads to a variation of the density of states $N(E_F)$ at the Fermi level, thus qualitatively explaining the drop of T_c for $x>x_{cr}$. In order to clarify if the T_c drop in $Y(Rh_{1-x}Ru_x)_4B_4$ is caused by the same mechanism, we studied in detail the structure of the valence-band spectra close to E_F for samples with different Ru content. The results are shown in Fig. 5(a). All spectra are normalized and aligned to the maximum of the transition-metal d-band emission. Similar to the behavior of $Ho(Rh_{1-x}Ru_x)_4B_4$ a clearly observable shift of E_F upon alloying Ru for Rh can be detected. To illustrate this analogy supplementary data for $Ho(Rh_{1-x}Ru_x)_4B_4$ are given in Fig. 5(b). Taking into account the experimental resolution, the pronounced shoulders at E_F observed for both bct systems with small values of x ($x\leq 0.10$) can only be explained if E_F is situated in a small peak which is separated from the main structure by a region of low

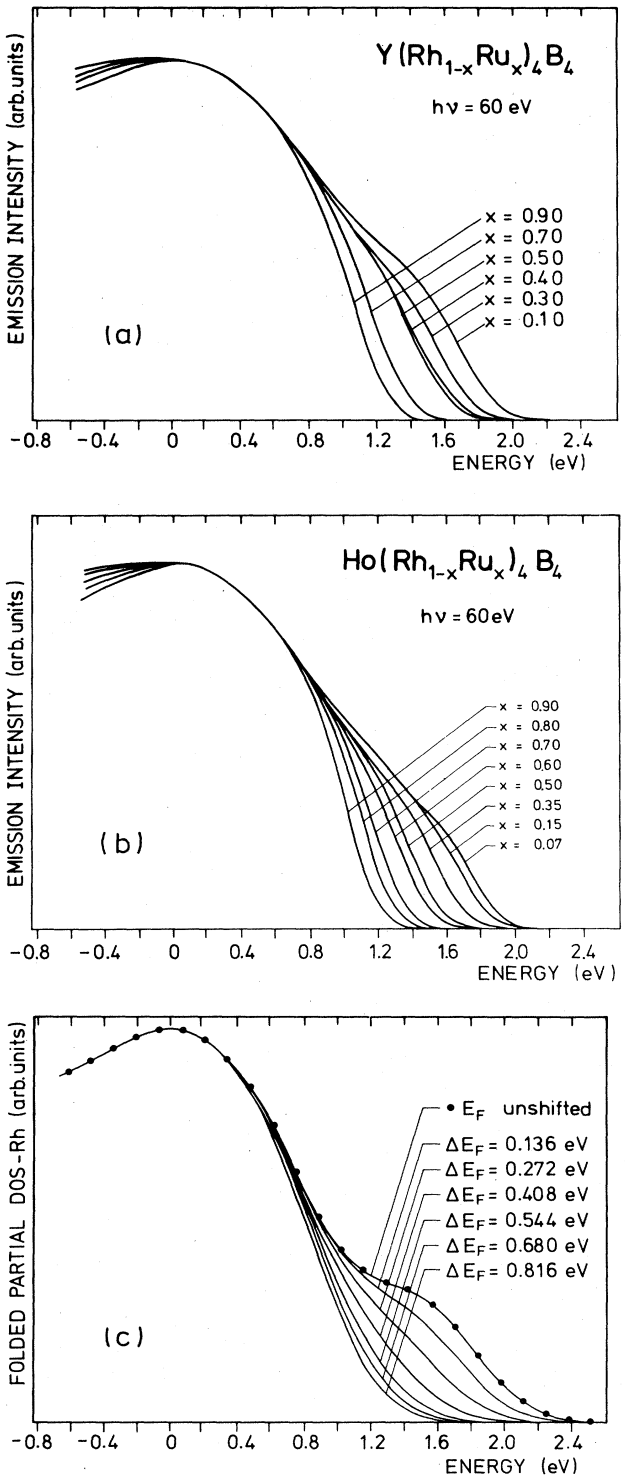

FIG. 5. (a) Photoemission spectra of the Fermi edge of $Y(Rh_{1-x}Ru_x)_4B_4$ for $h\nu=60$ eV. All spectra are aligned and normalized to the maximum of the transition-metal d-band emission. (b) Spectra for the related compound $Ho(Rh_{1-x}Ru_x)_4B_4$. (c) Calculated partial d-electron density of states for Rh in $HoRh_4B_4$ broadened by a Gaussian of 0.3 eV width. The position of E_F is successively shifted by ΔE_F to lower energies. The symbols correspond to the histogram bars of Fig. 3.

$N(E)$. The close similarity to the results of the band-structure calculations for pt $HoRh_4B_4$ provides additional justification to use it as a basis for the interpretation of this experiment.

As outlined in detail in Ref. 9, a substitution of Ru for Rh reduces the total number of d electrons, therefore shifting E_F to lower energies. For low Ru concentrations ($x<x_{cr}$) this shift leaves $N(E_F)$ within the resolution of the calculation nearly unchanged, as can be seen from Fig. 3, so that a nearly constant T_c is expected. Actually, this behavior is reflected in the superconducting phase diagram of Fig. 1. From an integration of the calculated partial density of states, it is obvious that for $x>0.40$ E_F enters a region of low $N(E)$ resulting in a drastical T_c decrease. After passing the valley in $N(E)$ according to the band-structure calculation a further increase of $N(E_F)$ should occur. Therefore superconductivity can be expected for samples with x values near 1. The data for YRu_4B_4 published in Ref. 8 and our measurements on the sample with $x=0.90$ prove this expectation, thus giving strong support for the explanation of the observed T_c behavior.

Although the energy resolution ($\Delta E=0.136$ eV) of the calculated electronic density of states is rather poor compared to the relevant shift of E_F ($\Delta E_F<1$ eV) due to the change of the electron concentration, and therefore the individual value of a single histogram bar should not be taken too seriously, we calculated within the framework of the model described above the $T_c(x)$ behavior. In order to do this on a finer x scale a superposition of three Gaussians was fitted to the calculated $N(E)$ histogram. This is shown for the total density of states in Fig. 6. T_c was calculated using McMillan's formula:[22]

$$k_B T_c=\frac{\hbar\langle\omega\rangle}{1.2}\exp\left[-\frac{1.04(1+\lambda)}{\lambda-\mu^*(1+0.62\lambda)}\right],$$

where for the mean phonon energy $\hbar\langle\omega\rangle=35,3$ meV and the Coulomb pseudopotential parameter $\mu^*=0.11$ was chosen for all values of x. For the electron-phonon coupling parameter λ, a starting value ($x=0.10$, $T_c=9.31$ K) of $\lambda_0=0.62$ was used in accordance with specific-heat measurements.[23] Furthermore, $\lambda\sim N(E_F)$ upon variation of x was assumed. In order to determine $N(E_F)$ for a given value of x the shift of E_F due to the change in valence-electron concentration was calculated by integrating the fitted density of states. The resulting $T_c^{calc}(x)$ curve obtained with the total density of states is shown in Fig. 7. There is a striking similarity to the experimental data of Fig. 1. The existing minor discrepancies for low values of x could be eliminated if the heights of the first and second histogram bars below E_F were changed less than $\pm5\%$, which may be within the numerical uncertainty. Figure 7 also correctly describes the reoccurrence of superconductivity for x values close to 1.

For the description of the substitution of Rh by Ru in terms of the band structure two extreme mechanisms are possible. Firstly, the reduction of d electrons only leads to changes in the occupation of the partial d-band density of states, which implies that the d-band structure is shifted in energy relative to the s and p bands to ensure a com-

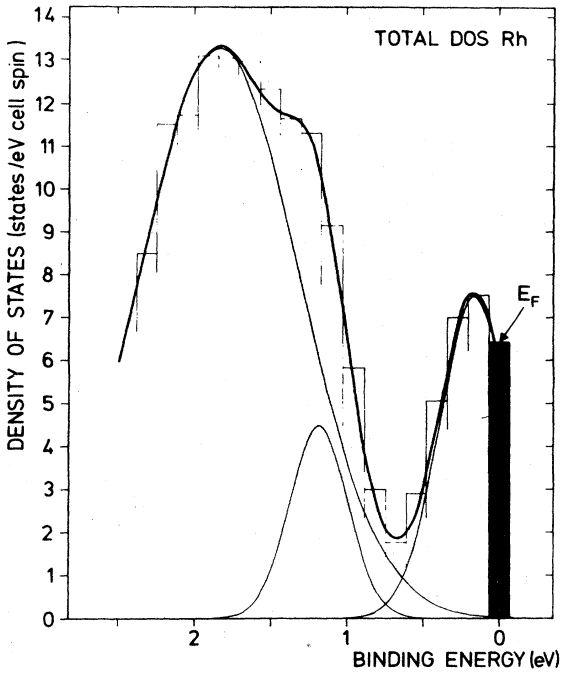

FIG. 6. Calculated total density of states $N(E)$ from Ref. 15 and the approximation of $N(E)$ by three Gauss peaks.

mon Fermi level throughout the sample. Secondly, the occupation of the total density is changed, which implies a variation in hybridization as d-band states are filled by s and p electrons. Presumably the actual behavior is within these two extreme limits, but it is not clear which mechanism prevails. Therefore the $T_c(x)$ calculation was carried out for both possibilities with qualitatively similar results. The agreement with the experimental $T_c(x)$ data is significantly better, especially for high values of x for the calculation using the total density of states for which the results are presented.

In order to demonstrate the effect of a shift of E_F on the valence-band spectra the position of the Fermi level in the calculated partial density of states of Fig. 3 has been successively shifted by ΔE_F (unit=10 mRy=0.136 eV).

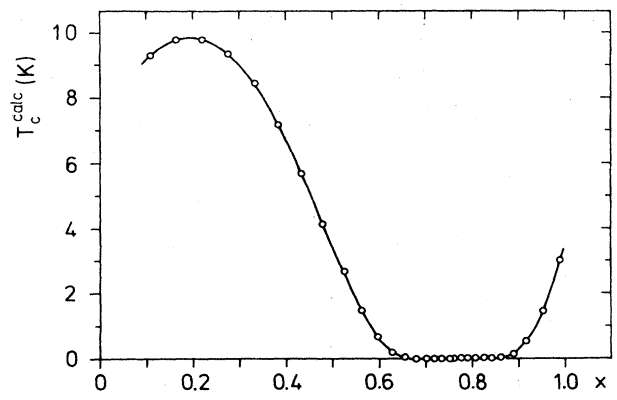

FIG. 7. Calculated superconducting critical temperature $T_c^{calc}(x)$ using McMillan's formula and the band-structure calculation of the total density of states.

In this case the partial density of states has to be used due to dominate d-band emission at $h\nu=60$ eV. The restricted experimental resolution was taken into account by finally folding with a Gaussian analyzer function with $\sigma=0.3$ eV. The results are shown in Fig. 5(c). Although the experimental structures are less pronounced, there is an excellent agreement between Figs. 5(a) and 5(c) as well as Figs. 5(b) and 5(c).

In previous Auger and photoemission (He I) studies on $Y(Rh_{1-x}Ru_x)_4B_4$ published by Hamaker *et al.*[16,17] the low T_c values for Ru-rich compound are attributed to the broadening of the d-band features due to the fact that the boron p states admix more strongly with Ru than Rh d states. A reduction of $N(E_F)$ and hence T_c was concluded from this broadening. However, this conclusion was drawn on the basis of overall band characteristics without special attention to E_F. In Fig. 8 photoemission spectra of the valence-band region of $Y(Rh_{1-x}Ru_x)_4B_4$ for different Ru content x are shown. To remove the contribution of inelastically scattered electrons the same background substraction procedure as in Fig. 2(a) was performed. Finally, all spectra were aligned and normalized with respect to the maximum of the transition-metal d-band emission. For clarity the changes near E_F outlined above are not shown. Upon substituting Ru for Rh not only a steady broadening of the lower d states and an increasing overlap with the boron p states is observed, but also for $x \geq 0.50$ the structures around the boron s_1 and s_2 states are strongly smeared out. However, even for the sample with $x=0.90$ the sharpness of the d band at $E_B=1.8$ eV seems nearly unchanged on this scale of binding energy, which is in contrast to the data of Refs. 16 and 17 where a strongly increasing overlap between their peaks at $E_B=1.7$ and 5.8 eV was found upon alloying. Moreover, these broadening effects which prove to be continuous can neither explain the sharp drop in T_c near $x=x_{cr}$ nor the recurrence of superconductivity for $x=0.90$.

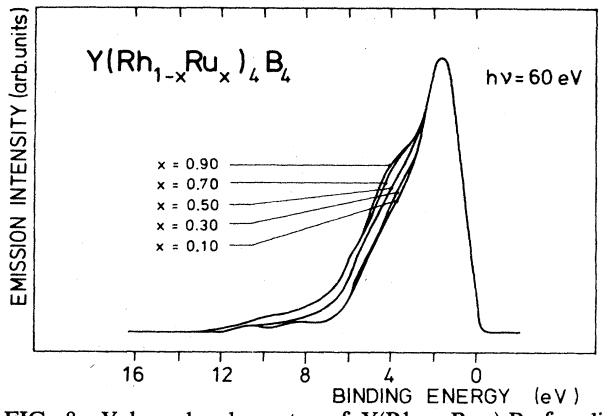

FIG. 8. Valence-band spectra of $Y(Rh_{1-x}Ru_x)_4B_4$ for different Ru content x. The same background subtraction procedure as in Fig. 2(a) was performed. All spectra are aligned and normalized with respect to the maximum of the transition-metal d-band emission. For clarity changes near the Fermi level due to the shift of E_F upon alloying are not shown.

IV. CONCLUSIONS

High-resolution photoemission measurements on the pseudoternary systems $R(Rh_{1-x}Ru_x)_4B_4$ (R = Y,Ho) clearly indicate a shift of E_F to lower energies in case of substituting Ru for Rh. This behavior was found for magnetic Ho ions occupying the R sublattice[9] as well as for nonmagnetic Y. From a comparison with band-structure calculations for the primitive-tetragonal modification of the structure type variations of $N(E_F)$ connected with this shift prove to be the underlying mechanism for T_c suppression and in case of $Y(Rh_{1-x}Ru_x)_4B_4$ the reoccurrence of superconductivity for high x values. We expect that this shift of E_F and the related changes in $N(E_F)$ and hence T_c occur in all pseudoternary boride systems where Rh is substituted by Ru. Contrary to this our earlier results with pt $Ho(Rh_{1-x}Ir_x)_4B_4$ (Ref. 4) where the number of valence electrons is constant, clearly show that such a shift of E_F to lower energies does not exist. As outlined above in this case the origin of the T_c suppression is a pronounced broadening of the d-band structure with x. Hence, although the superconducting phase diagrams of the compound series $R(Rh_{1-x}Ru_x)_4B_4$ and $R(Rh_{1-x}Ir_x)_4B_4$ are rather similar in shape, quite different mechanisms are responsible for the reduction of the superconducting critical temperature T_c.

ACKNOWLEDGMENTS

We thank the staff of the Hamburger Synchrotronstrahlungslabor (HASYLAB), Hamburg, Germany, for their kind hospitality and technical assistance during the photoemission measurements. Part of this work was supported by the Bundesminister für Forschung und Technologie (Germany).

[1] *Superconductivity in Ternary Compounds II,* edited by M. B. Maple and Ø. Fischer (Springer, Berlin, 1982).

[2] *Superconductivity in Magnetic and Exotic Materials,* Vol. 52 of *Springer Series in Solid State Sciences,* edited by T. Matsubara and A. Kotani (Springer, Berlin, 1984).

[3] H. C. Ku, in *Proceedings of the 17th International Conference on Low Temperature Physics—LT-17,* edited by U. Eckern, A. Schmid, W. Weber, and H. Wühl (North-Holland, Amsterdam, 1984), p. 105.

[4] R. Knauf, R. Müller, H. Adrian, G. Saemann-Ischenko, and R. L. Johnson, in *Proceedings of the 17th International Conference on Low Temperature Physics—LT-17,* edited by U. Eckern, A. Schmid, W. Weber, and H. Wühl (North-Holland, Amsterdam, 1984), p. 97.

[5] H. E. Horng and R. N. Shelton, in *Ternary Superconductors,* edited by G. K. Shenoy, B. D. Dunlap, and F. Y. Fradin (North-Holland, New York, 1981), p. 213.

[6] Y. Muto, H. Iwasaki, T. Susaki, N. Kobayashi, M. Ikebe, and M. Isino, in *Ternary Superconductors,* edited by G. K. Shenoy, B. D. Dunlap, and F. Y. Fradin (North-Holland, New York, 1981), p. 197.

[7] D. C. Johnston, Solid State Commun. **24**, 699 (1977).

[8] R. N. Shelton, H. E. Horng, A. J. Bevelo, J. W. Richardson, R. A. Jacobson, S. D. Bader, and H. C. Hamaker, Phys. Rev. B **27**, 6703 (1983).

[9] R. Knauf, A. Thomä, H. Adrian, and R. L. Johnson, Phys. Rev. B **29**, 2477 (1984).

[10] R. L. Johnson and J. Reichardt, Nucl. Instrum. Methods **208**, 791 (1983).

[11] R. Müller, A. Thomä, T. Theiler, H. Adrian, G. Saemann-Ischenko, and M. Steiner, in *Proceedings of the 17th International Conference on Low Temperature Physics—LT-17,* edited by U. Eckern, A. Schmid, W. Weber, and H. Wühl (North-Holland, Amsterdam, 1984), p. 99.

[12] P. Steiner, H. Höchst, and S. Hüfner, Z. Phys. B **30**, 129 (1978).

[13] T. Jarlborg, A. J. Freeman, and T. J. Watson-Yang, Phys. Rev. Lett. **39**, 1032 (1977).

[14] A. J. Freeman and T. Jarlborg, J. Appl. Phys. **50**, 1876 (1979).

[15] A. J. Freeman and T. Jarlborg, in *Superconductivity in Ternary Compounds II,* edited by M. B. Maple (Springer, Berlin, 1982), pp. 167ff.

[16] H. C. Hamaker, S. D. Bader, G. Zajac, R. N. Shelton, A. J. Bevelo, and H. E. Horng, Solid State Commun. **48**, 589 (1983).

[17] H. C. Hamaker, G. Zajac, and S. D. Bader, Phys. Rev. B **27**, 6713 (1983).

[18] N. V. Smith, G. K. Wertheim, S. Hüfner, and M. M. Traum, Phys. Rev. B **10**, 3197 (1974).

[19] H. Ishii, T. Miyahara, T. Hanyu, and S. Yamaguchi, J. Phys. Soc. Jpn. **53**, 2151 (1984).

[20] H. Höchst and M. K. Kelly, Phys. Rev. B **30**, 1708 (1984).

[21] J. H. Weaver, C. Krafka, D. W. Lynch, and E. E. Koch, in *Physics Data* (ZAD, Karlsruhe, 1981), Vol. 18-2.

[22] W. L. McMillan, Phys. Rev. **167**, 331 (1968).

[23] H. Adrian, R. Müller, and R. Behrle, Phys. Rev. B **26**, 2450 (1982).